

BEAM INDUCED FLUORESCENCE MONITORS

F. Becker*, GSI, Darmstadt, Germany

Abstract

Non-intersecting diagnostic devices in hadron accelerators offer continuous online monitoring capability. They also avoid the problem of potential thermal damage in high-current applications. Taking advantage of the residual gas as active material, the Beam Induced Fluorescence (BIF) monitor exploits gas fluorescence in the visible range for transversal profile measurements. Depending on beam parameters and vacuum-constraints, BIF monitors can be operated at base-pressure or in dedicated local pressure bumps up to the mbar range. Nowadays, BIF monitors are investigated in many accelerator laboratories for hadron energies from about 100 keV up to several 100 GeV. This paper gives an introduction to the measurement principle and typical operating conditions. It summarizes recent investigations, e.g. on different working gases, and it compares various technical realizations.

DEVELOPMENT OF THE METHOD

Systematic investigation of the fluorescence mechanism in gases was matter of particular interest already during the first half of the twentieth century and pursued by atomic physics researchers [1, 2]. Experiments were closely connected to the development of spectrographs, light sources for absorption spectroscopy and dedicated excitation drivers like spark discharge, electron guns or ion sources. A 200 keV proton beam as excitation driver was used to measure optical spectra and to determine absolute electron capture and loss cross-sections in a $3 \cdot 10^{-2}$ mbar nitrogen atmosphere [3]. Beside the main cross section results and spectral data, the influence of secondary electrons on the observed optical transitions and their appearance as a beam halo was discussed.

The first beam induced fluorescence monitors as dedicated systems for beam diagnostics have been realized at the LEBT-section of the PSI cyclotron facility for 60 to 870 keV ions [4, 5] and at the 6.7 MeV low energy demonstration accelerator (LEDA) in Los Alamos [6, 7]. At PSI, the monitor was realized with a stepper controlled, tilting PMT slit detector and was operated at $\leq 10^{-6}$ mbar base pressure. At LANL, transverse beam profiles were successfully obtained from projections of fluorescence images in $\leq 10^{-5}$ mbar nitrogen gas with an intensified video camera. Additionally, the monitor was equipped with a pulsed leak valve. Within the last two decades, fundamental investigations were carried out [8, 9, 10, 11] and BIF monitors have been successfully commissioned in synchrotrons [12, 13, 14] and linear accelerators or transport sections

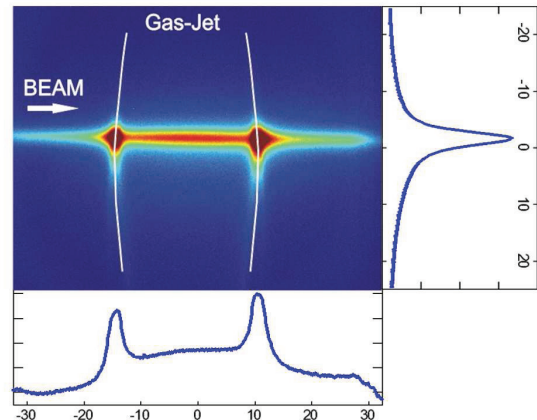


Figure 1: Fluorescence image of a 12 mA, 100 μ s Ar^+ -beam crossing a supersonic nitrogen gas jet in the UNILAC gas stripper. Projections along (transverse beam profile) and across the beam path are given in arbitrary intensity units and millimeter length. Due to the stripping of Ar in the gas jet, the signal increases along the beam direction.

Table 1: Collection of BIF-monitors realized at different laboratories. If monitors are used as standard operating tool the lab is marked with (*). Corresponding references, type of accelerator (L = linac, S = synchrotron, LEBT/HEBT transport sections) and specialties are referred likewise.

Lab.	Ref.	Acc.	Specialty
PSI*	[4, 5]	LEBT	Reliable design
LANL	[6, 7]	HEBT	Pulsed valve
IPN	[9, 15]	L	Doppler spectr.
CERN	[8, 12]	S	Highest energy
GSI*	[10, 29, 26]	L, HEBT	Spectr. var. ions
COSY*	[13, 32]	S	PMT-array
BNL*	[14]	S	H gas jet
CIEMAT	[20]	L	Rad. tolerant
IAP	[28]	L	Tomography

[5, 15, 16, 17, 18, 19]. Meeting the increasing demands for online diagnostics in upcoming accelerators, many innovative enhancements of the BIF method are currently being developed [20, 14, 21]. A collection of BIF-monitors realized at different laboratories is given in Table 1. In the following, a systematic overview is presented and references are listed according to specific aspects of the method.

MEASUREMENT PRINCIPLE

BIF monitors rely, like Ionization Profile Monitors (IPMs), on the interaction of beam ions with any working gas, residual or specifically introduced. The differen-

*Frank.Becker@gsi.de

tial energy loss of beam ions is the driver for ionization and excitation of the working gas and the beam itself [15]. This paper focuses on the fluorescence of different working gases, due to its universal area of application for almost any kind of ion beams. As long as we might assume the locations of exciting beam ions and the emitting gas atoms or molecules to be nearly identical, fluorescence light can be used to image the beam particle distribution. A sensitive, spatially resolving photo detection system is used for fluorescence imaging, e.g. intensified cameras or PMT-arrays.

ESTIMATION OF SIGNAL STRENGTH

The sensitivity is either determined by the number of detected ionized gas atoms or electrons (IPM), or the number of detected beam induced fluorescence photons (BIF). In the following, we consider both monitors to be intensified in a way that they are operated in a particle counting mode. Cross sections for gas ionization by proton beams [22] and generation of fluorescence photons [8, 12] have been experimentally determined. It was shown that cross sections scale with the differential energy loss for particle energies from 100 keV to 450 GeV.

In this representation, cross-sections contain beam parameters like particle energy E and effective charge \bar{q} . In low gas densities and for large impact parameters the effective charge $\bar{q} = Z_{projectile} - \bar{n}_e$, with \bar{n}_e the number of remaining electrons. For any particle beam the number of detected ions Y_{ionize} or fluorescence photons Y_{photon} is determined by the number of beam ions N_{Ion} per integration time, the gas density ρ , the length of the observed beam gas interaction volume Δs , the probability for single event detection $P_{Detector}$ and the corresponding cross sections σ_{ionize} or σ_{photon} , see Equations (1) & (2). They can be scaled for heavy ion beams according to Equation (3).

$$Y_{ionize} = N_{Ion} \rho \Delta s P_{Det.} \sigma_{ion.}(E, \bar{q}) \quad (1)$$

$$Y_{photon} = N_{Ion} \rho \Delta s P_{Det.} \sigma_{phot.}(E, \bar{q}) \Omega \quad (2)$$

$$\sigma_{ion./phot.} \propto \left(\frac{dE}{dx} \right) \Rightarrow \sigma_{ion./phot.} \propto \bar{q}^2 \quad (3)$$

The average energy \bar{W}_{ionize} which is required to produce an electron-ion-pair in gas only depends on the gas species, neither on the ion species nor the ion energy and is in the order of 30 eV (34.8 eV for N_2) [23]. In Bethe-Bloch formula's energy-range of validity, \bar{W}_{ionize} is rather constant. Therefore Y_{ionize} and accordingly σ_{ionize} scale with the differential energy loss [24]. Further it was shown that \bar{W}_{ionize} is sensitive to trace amounts of various gas-contaminants. For projectile velocities at particle energies $E \leq 100$ keV/u the value of \bar{W}_{ionize} increases [25].

Very similar to gas-ionization, the fluorescence process requires an average energy \bar{W}_{photon} to produce an optical photon, according to Equation (4).

$$\bar{W}_{photon} = \bar{W}_{ionize} \cdot \frac{\sigma_{ionize}(E, \bar{q})}{\sigma_{photon}(E, \bar{q})} \quad (4)$$

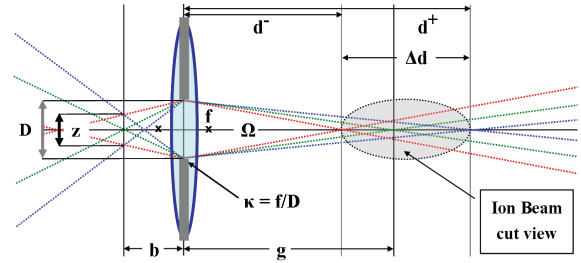


Figure 2: Schematic drawing of the BIF optical layout.

\bar{W}_{photon} was experimentally determined to be several keV in nitrogen [3, 8]. In residual nitrogen gas, the energy converted into fluorescence photons is rather constant and about 1% of the differential energy loss, within a spectral range from 400 to 700 nm [11]. It is also sensitive to the gas species and impurities, see [26]. However, for given gas and beam settings, cross sections σ , and number of beam ions N per integration time are preset parameters.

PHOTO DETECTION SYSTEM

According to Equation (2), the detection system can be optimized regarding the geometrical parameters Δs , the solid angle Ω and the probability for photon detection $P_{Detector}(\lambda)$, including losses in the optical components.

Optical Layout

The optical system images the fluorescence object onto the sensor with the required scaling factor. Another boundary condition is the optical depth of field Δd , that should cover not less than the beam diameter, see Fig. 2. Equations (5) and (6) give the deviations $g - d^-$ and $d^+ - g$ with respect to the object distance g , the focal length f , the f-number κ and the diameter of the allowed blurring circle z , that is typically in the order of the pixel size. For a given geometry and z , the depth of field increases with increasing f-numbers. Nevertheless, the solid angle Ω scales like $\propto \kappa^{-2}$, with an associated signal loss.

$$g - d^- = \frac{g(g-f)}{d_h + (g-f)}; \quad d^+ - g = \frac{g(g-f)}{d_h - (g-f)} \quad (5)$$

$$\text{with } d_h = \frac{f^2}{\kappa z} + f \quad (6)$$

The spectral transmission of the lenses and optical components can be optimized as well and should cover the spectral lines of interest. Spherical aberrations of purchased lenses are typically well specified and minor issues. However, chromatic aberrations are critical for UV-enhanced quartz lenses. Perspective aberrations and the relative spread in contributing solid angle increase with increasing beam diameters. For $g = 200$ mm, $f = 16$ mm, $\kappa = 1.4$ and a Gaussian beam of $\sigma_x \cdot \sigma_y = 30 \times 30$ mm², the relative error in measured beam width $\Delta\sigma/\sigma = 12,2\%$. Quasi-parallel projections as realized in telecentric lenses overcome this issue at the expense of light intensity.

Table 2: Collection of common detection systems, sorted by pixel arrangement. Known advantages and disadvantages are listed, as well as corresponding references where the system has been realized, with further information.

AREA SCAN			
Device	QE %	Pros	Cons
ICCD [6, 9, 10]	5-20	+ ns-gating + low noise	- low QE - rad. sensit.
ICID [20]	5-20	+ ns-gating + dynamics + rad. tolerant	- low QE - resolution - noise
EMCCD [29]	40-90	+ high QE + high resol.	- slow gating - rad. sensit.
LINE SCAN			
PMT-array [30, 20]	10-40	+ fast resp. + low noise	- ADC issue - low resol.
Array of SiPMs	40-90	+ high QE + fast resp.	- ADC issue - noise
SINGLE PIXEL			
PMT [4, 8] or SiPM	10-90	+ robust + low noise	- mechanics - step motor

Optical Detector

The detector system determines spectral acceptance and detection probability $P_{Detector}(\lambda)$ due to its characteristic quantum efficiency $QE(\lambda)$. Depending on the amount of photons per integration time at the detector, different realizations are possible. In Table 2 a collection of common detection systems is presented.

Scientific CCD or CMOS cameras have QEs from 30 to 90 % and require about 5 to 100 photons per pixel for a detectable signal above the noise floor. Figure 1 shows a fluorescence image of a 1,4 MeV/u, 12 mA, 100 μs Ar⁺-beam in an inhomogeneous supersonic nitrogen gas jet, recorded with a standard VGA CCD camera.

For decreasing Y_{photon} the noise contribution has to be reduced by cooling or by connecting an image intensifier to a standard camera [10]. The system can be operated in a photon counting mode, that even single photons are detected upon the inherent noise. Figure 3 shows single fluorescence photons of a 4.7 MeV/u, 1 mA, 500 μs Xe²¹⁺-beam in $5 \cdot 10^{-6}$ mbar N₂ gas, recorded with a chevron ICCD. Photon counting capability and adequate QE in the observed spectral range is recommended for all BIF applications to reduce integration time and required gas load.

Compared to PMTs or solid state amplifiers, systems with MCP-based image intensifiers have inferior QE , due to MCP open area ratios of about 50 %. In addition to the investigated systems, silicon photo multipliers (SiPM) with a performant multichannel ADC seem to be a promising alternative [31]. Most BIF monitors are realized with area or line scan detectors, recording transverse x/y-projections. Some groups work on reconstruction of 2-D beam distributions by tomography techniques [27, 28].

CHOICE OF WORKING GAS

Pressure and working gas species determine ρ and σ_{photon} . Therefore, they have a crucial impact on the photon yield Y_{photon} , see Equation (2). According to the specifications for installations in a specific vacuum system, the monitor must be either operated at base pressure, or it is allowed to introduce a dedicated working gas. At base pressure the residual gas is a composition of many species and usually H₂ dominated in UHV-systems and N₂ dominated in clean HV-systems with $p \geq 10^{-9}$ mbar. In the following, dedicated working gases will be discussed.

Displacement Error and Fluorescence Lifetime

Fluorescence imaging is an indirect method and measurement errors due to displacement of gas atoms have to be taken into account. The displacement is determined by thermal motion, momentum transfer, dissociation of molecules and acceleration of charged gas ions in the electrical field of the ion beam [8, 29]. Highest accuracy can be achieved, using heavy gas species with short fluorescence lifetimes. Fluorescence halos due to excitation by secondary electrons can be avoided by spectral selection, because relevant cross sections drop for ionized gases, e.g. N₂⁺, Xe⁺ [18].

Imaging Spectroscopy and Light Yield

With an imaging spectrograph, coupled to a trialkali ICCD (300-800 nm) beam profile data was assigned to optical transitions [26]. Inert gases (He, Ne, Ar, Kr, Xe) have been chosen due to their atomic occurrence (no dissociation dynamics) and short fluorescence lifetimes ≤ 10 ns. N₂-gas as dominating species in clean HV -installations was chosen as a reference. After normalization, all investigated gases but He show identical beam profiles and suitable optical transitions. Normalized with respect to the gas pressure and the differential energy loss, the integral nitrogen signal was about four times higher than the signal observed in rare gases, for different investigated ion species and charge states. In principle, fluorescence spectra of specific gases did not change with the ion species (p, S⁶⁺, Ni⁹⁺, Ta²⁴⁺, U²⁸⁺) [26].

Gas Dosing Systems

Beside operation with a gas mixture at base pressure [5], a regulated leak valve provides slow controlled pressure bumps along a constantly pumped beam line and defines the parameters of a dedicated working gas [19]. Remote controlled types with motorized needle and pressure controlled feedback system provide constant gas pressures. For transport sections with low duty cycle or sporadic monitoring, a pulsed valve is an alternative. Triggered solenoid and piezoelectric valves provide down to ms gas puffs

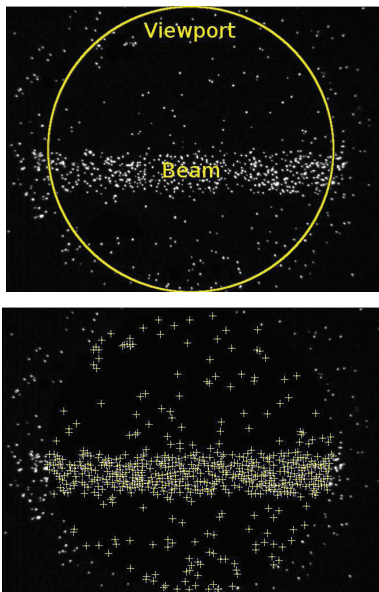


Figure 3: 8-bit VGA fluorescence image (upper) with a selected region of interest (yellow circle). The lower part show the analyzed image with detected local grayscale-maxima. The 'Maxima'-algorithm of the image processing tool 'ImageJ' assigns an index to each spot (yellow crosses). Result is 603 counts within the ROI.

[7, 32] and allow BIF operation even in synchrotron vacuum conditions. Low duty-cycles and lower mean pressures allow for higher peak pressures and increased fluorescence count rates. Directed gas jets as depicted in Fig. 1 combine gas densities of up to 10^{-3} mbar equivalent pressure with low gas contamination of the vacuum system. [14, 21]. Some installations exploit the beam induced gas desorption and fluorescence [17].

THE LIMITING FACTORS

Compared to IPMs, BIF monitors have to cope with about a factor of thousand lower cross sections σ_{photon} , depending on the database [8, 12]. Additionally, the required depth of field limits the F-number to $\kappa \geq \kappa(\Delta d)$, with typical solid angles $\Omega \leq 10^{-3}$. All this reduces the Photon yield Y_{photon} . If the monitor has to be operated at low gas pressures with a small number of ions per integration time and ion energies near the ionization minimum, even high QE sensors with photon counting capability will run into shot noise issues. The 603 detected events from Figure 3 are sufficient to determine beam profiles of a Gaussian distribution. For less than ≈ 30 counts, the χ^2 -method fails. Binning of detector pixels improves statistical fluctuations at the cost of spatial resolution. Non-Gaussian density distributions require a larger number of detected photons. In general, the error σ_μ and σ_σ in statistical moments μ and σ scale with the number of counts $n = Y_{\text{photon}}$, see Eq. (7).

$$\sigma_\mu \propto \frac{1}{\sqrt{n}} \quad \wedge \quad \sigma_\sigma \propto \frac{1}{\sqrt{2n}} \quad (7)$$

Radiation due to beam losses or decay of produced particles is another limiting factor. We found that beam induced radiation background is detected with different intensified camera systems [29]. This contribution increases with the ion energy and reduces the actual dynamic range of the intensified camera system. Therefore, effective shielding and radiation hard components should be foreseen [20].

CONCLUSION

BIF monitors have undergone noteworthy development in many technical aspects but especially in the optical read-out systems with on-board ADC and user-friendly interfaces. They became standard diagnostics in a still growing number of accelerator labs. In comparison to other profile monitors, like SEM-grids, wire scanners or IPMs, profiles recorded with BIF monitors are in excellent agreement [4, 9, 16, 33]. Although technical challenges have to be taken up, BIF monitors are operated at minimal ionization energy with single photon counting and pulsed valves, in radiation harsh environment with appropriate shielding and even in synchrotron vacuum conditions with the help of gas jets.

ACKNOWLEDGEMENTS

I thank all colleagues who supported this contribution with their specific information and ideas. Furthermore, I want to express my special thanks to Peter Forck and the colleagues from GSI beam diagnostics department.

REFERENCES

- [1] G. Herzberg and J. Spinks, *Atomic spectra and atomic structure*. New York: Dover Publications, 1944.
- [2] G. Herzberg, *Molecular spectra and molecular structure*. Toronto, New York - van Nostrand, 1950.
- [3] R.H. Hughes and J.L. Philpot, "Spectra induced by 200-keV proton impact on nitrogen," *Physical Review*, vol. 123, pp. 2084–2086, 1961.
- [4] L. Rezzonico, "Beam diagnostics at SIN," in *11th Int. Conference on Cyclotrons and their Applications, Tokyo*, pp. 457–460, PSI, 1987.
- [5] L. Rezzonico, U. Frei, M. Graf, and R. Erne, "A profile monitor using residual gas," in *12th International Conference on Cyclotrons and their Applications, Berlin*, pp. 313–316, PSI, 1989.
- [6] D.P. Sandoval, R.C. Garcia, J.D. Gilpatrick, M.A. Shinas, R. Wright, V. Yuan, and M.E. Zander, "Fluorescence-based video profile beam diagnostics: Theory and experience," in *BIW, Santa Fe*, 319, pp. 273–282, 1993.
- [7] J.H. Kamperschroer, J.D. Gilpatrick, P.A. Gurd, D.W. Madson, D.G. Martinez, J.F.O. Harad, J. Sage, T.L. Schaefer, R.B. Shurter, and M.W. Stettler, "Initial operation of the LEDA beam-induced fluorescence diagnostic," in *AIP Conf. Proc.*, Vol. 319 - LA-UR-00-2361, pp. 273–282, LANL, Oct. 1996.
- [8] M.A. Plum, E. Bravin, J. Bossler, and R. Maccaferri, "N2 and Xe gas scintillation cross-section, spectrum, and lifetime measurements from 50 MeV to 25 GeV at the CERN

- PS and booster,” *Nuclear Instruments and Methods in Physics Research Section A*, Vol. 492, no. 1–2, pp. 74–90, 2002.
- [9] P. Ausset, S. Bousson, D. Gardès, A.C. Mueller, B. Pottin, R. Gobin, G. Belyaev, and I. Roudskoy, “Optical Transverse Beam Profile Measurements for High Power Proton Beams,” in *EPAC2002, Paris*, THPRI066, pp. 1840–1842, JACoW, 2002.
- [10] P. Forck and A. Bank, “Residual Gas Fluorescence For Profile Measurements at the GSI UNILAC,” in *EPAC2002, Paris*, THPRI056, pp. 1885–1887, JACoW, 2002.
- [11] F. Becker and P. Forck, “Beam Induced Fluorescence (BIF) Monitor for Transverse Profile Determination of 5 to 750 MeV/u Heavy Ion Beams,” in *DIPAC2007, Venice*, M003A02, pp. 33–35, JACoW, 2007.
- [12] A. Variola, R. Jung, and G. Ferioli, “Characterization of a nondestructive beam profile monitor using luminescent emission,” *Phys. Rev. Special Topics - Accelerators and Beams*, Vol. 10, pp. 1–14, August 2007.
- [13] J. Dietrich et al., “Non-destructive Beam Position and Profile Measurements Using Light Emitted by Residual Gas in a Cyclotron Beam Line,” in *EPAC2008, Genova*, TUPC022, pp. 1095–1097, JACoW, 2008.
- [14] T. Tsang, S. Bellavia, R. Connolly, D. Gassner, Y. Makdisi, T. Russo, P. Thieberger, D. Trbojevic, and A. Zelenski, “Optical beam profile monitor and residual gas fluorescence at the RHIC polarized hydrogen jet,” *Review of Scientific Instruments*, Vol. 79, pp. 105103–105103–12, 2008.
- [15] P. Ausset, S. Bousson, D. Gardes, A.C. Mueller, B. Pottin, R. Gobin, G. Belyaev, and I. Roudskoy, “Transverse Beam Profile Measurements for High Power Proton Beams,” in *EPAC2002, Paris*, THGB003, pp. 245–247, JACoW, 2002.
- [16] P. Forck, A. Bank, T. Giacomini, and A. Peters, “Profile monitors based on residual gas interaction,” in *DIPAC2008, Lyon*, ITTA01, pp. 223–227, JACoW, 2005.
- [17] F.M. Bieniosek, S. Eylon, P. Roy, and S. Yu, “Optical Faraday Cup for Heavy Ion Beams,” in *PAC2005, Knoxville, Tennessee*, RPAT022, pp. 1805–1807, JACoW, 2005.
- [18] D. Varentsov et al., “Transverse optical diagnostics for intense focused heavy ion beams,” *Contributions to Plasma Physics*, Vol. 48, pp. 586–594, October 2008.
- [19] C. Andre, F. Becker, H. Brauning, P. Forck, R. Haseitl, and B. Walasek-Hoehne, “Beam Induced Fluorescence (BIF) monitors as a standard operating tool,” in *DIPAC2011, Hamburg*, M0PD60, JACoW, 2011.
- [20] J.M. Carmona et al., “First measurements of non-interceptive beam profile monitor prototypes for medium to high current hadron accelerators,” in *HB2010, Morschach, Switzerland*, WE01C04, pp. 502–505, JACoW, 2010.
- [21] M. Putignano and C. Welsch, “Optimization studies of planar supersonic gas-jets for beam profile monitor applications,” in *IPAC2010, Kyoto*, M0PE073, pp. 1149–1151, JACoW, 2010.
- [22] M.E. Rudd, R.D. DuBois, L.H. Toburen, and C.A. Ratcliffe, “Cross section for ionization of gases by 5–4000-keV protons and for electron capture by 5–150-keV protons,” *Physical Review A*, vol. 28, pp. 3244–3257, December 1983.
- [23] W.R. Leo, *Techniques for Nuclear and Particle Physics Experiments*. Springer Berlin, 1994.
- [24] G.F. Knoll, *Radiation Detection and Measurement*. Wiley & Sons, fourth ed., August 2010.
- [25] P. Christmas, “Average energy required to produce an ion pair : Icru report 31, 1979, ICRU publications, po box 30165, washington, dc 20014, u.s.a. 52 pp. £5.25.,” *Radiation Physics and Chemistry (1977)*, vol. 16, no. 6, pp. 493–493, 1980.
- [26] F. Becker, F.M. Bieniosek, P. Forck, R. Haseitl, A. Hug, P. Ni, D. Hoffmann, and B. Walasek-Hoehne, “Beam Induced Fluorescence Monitor & Imaging Spectrography of Different Working Gases,” in *DIPAC2009, Basel*, TUPB02, pp. 161–163, JACoW, 2009.
- [27] G. Belyaev, I. Roudskoy, D. Garde, P. Ausset, and A. Olivier, “Tomography reconstruction of the intensity distribution in a beam cross-section using optical diagnostics,” *Nuclear Instruments and Methods in Physics Research A*, Vol. 578, pp. 47–54, May 2007.
- [28] H. Reichau, O. Meusel, and U. Ratzinger, “Estimation of profile width in hybrid ion beam tomography,” in *BIW2010, Santa Fe*, TUP5M059, pp. 292–296, JACoW, 2010.
- [29] F. Becker, C. Andre, F.M. Bieniosek, P. Forck, P.A. Ni, and D.H.H. Hoffmann, “Beam Induced Fluorescence (BIF) Monitor for Intense Heavy Ion Beams,” in *BIW2008, Lake Tahoe*, TUPTPF054, pp. 339–343, JACoW, 2008.
- [30] J. Dietrich, C. Boehme, T. Weis, A.H. Botha, J.L. Conrady, and P.F. Rohwer, “Beam Profile Measurements Based on Light Radiation of Atoms Excited by the Particle Beam,” in *PAC2007, Albuquerque*, FRPMN020, pp. 3955–3957, JACoW, 2007.
- [31] D. Liakin, S. Barabin, A. Orlov, P. Forck, and T. Giacomini, “A Counting Module for an Advanced Ionization Profile Monitor,” in *EPAC2008, Genoa*, TUPC060, pp. 1094–1096, JACoW, 2008.
- [32] V. Kamerzhiev, J. Dietrich, F. Klehr, and K. Reimers, “Progress with the Scintillation Profile Monitor at COSY,” in *DIPAC2011, Hamburg*, M0PD51, JACoW, 2011.
- [33] J. Egberts, P. Abbon, F. Jeanneau, J. Marroncle, J.-P. Mols, T. Papaevangelou, F. Becker, P. Forck, and B. Walasek-Hoehne, “Detailed Experimental Characterization of an Ionization Profile Monitor,” in *DIPAC2011, Hamburg*, WE0A03, JACoW, 2011.